IEEE Access
Multidisciplinary ⋮ Rapid Review ⋮ Open Access Journal

Received November 27, 2019, accepted December 23, 2019, date of publication December 30, 2019,
date of current version January 8, 2020.

*Digital Object Identifier 10.1109/ACCESS.2019.2962908*

# Stress-Induced Magnetic Anisotropy Model Under Unidirectional Tension

**FUCHEN ZHANG[1,2], HONGMEI LI[2], CHENGXIANG SHI[2], AND RUIQING JIA[1]**
[1]School of Mechanical Electronic and Information Engineering, China University of Mining and Technology (Beijing), Beijing 100083, China
[2]School of Mechanical Engineering, North Minzu University, Yinchuan 750021, China

Corresponding author: Hongmei Li (lihongmei@nun.edu.cn)

This work was supported by the National Natural Science Foundation of China under Grant 51367001 and Grant 51507005.

**ABSTRACT** In this paper, we theoretically investigated stress-induced magnetic anisotropy and presented a model based on a unidirectional tensile stress experiment. Firstly, the theoretical model was simulated based on the work of Jiles. Secondly, experiments were conducted, and data under unidirectional tensile stress were collected and analyzed. Finally, the model was developed by correlating the experimental data and theoretical model. Our model provides a good description of stress-induced magnetic anisotropy under unidirectional tensile stresses and lays down a foundation for the quantitative testing and evaluation of stress of ferromagnetic materials through the magnetic method.

**INDEX TERMS** Magnetomechanical effect, stress-induced magnetic anisotropy model, stress testing.

## I. INTRODUCTION

Ferromagnetic steels are widely used in manufacturing the key mechanical components and in petroleum, chemical, mining, and other industries because of their excellent mechanical properties. In the service and manufacture of components, mechanical damages are the most critical factors affecting the safety of structures. The detection and evaluation of stress state of ferromagnetic steel structures are important because most mechanical damages are closely related to stress. Stress testing and evaluation technologies using the magnetic method have recently attracted attention due to their simple and convenient application [1]–[5].

The magnetomechanical effect is the physical mechanism underlying magnetic stress testing. Jiles and Atherton [1] established a model (J-A model) to explain magnetomechanical relationship on the basis of the approach law and effective field theory. The J-A model builds a quantitative relationship between stress and magnetization [6]. A series of analyses of the relationships between the stress of ferromagnetic materials and surface magnetic field signals was performed based on this model [7]–[11]. Li and Xu [12]–[14] modified the J-A model to provide an accurate description of magnetic properties under tension and compression. Moreover, the modified J–A model can be used to describe metal magnetic memory (MMM) mechanism in elastic stress stage and analyse MMM field changes at fatigue process. Shi *et al.* [15]–[17] established several magnetomechanical models that correlate stress with the surface magnetic signals of stress concentration zone. The proposed theoretical model can predict the MMM signals in a complex environment a nonlinear coupled model is proposed to improve the quantitative evaluation of the magnetomechanical effect. This theoretical model can be adopted to quantitatively analyze magnetic memory signals. It is found that the magnetic output is different when the stress direction and the magnetic field direction are different. Cullity observed that when stress is applied in the direction of the external magnetic field for low-carbon alloy steel, magnetization is enhanced by tensile stress but weakened by compressive stress [18]. Yang *et al.* [19] studied the influence of stress and external magnetic field on the residual magnetic field of ferromagnetic steel and found that the direction of the residual magnetic field is affected by the combined action of stress and external magnetic field. They also reconstructed the magnetization inside the structure by using surface magnetic field signals and found that stress-induced magnetization under geomagnetic field is directed along the stress and the intensity of the stress-induced magnetization is linearly related to the applied stress [20]–[22]. Sun *et al.* found that stress-induced magnetic anisotropy is represented by stress dependence of magnetic permeability in different directions [23]. Although numerous works were conducted and many substantial results were obtained in this field, verification studies that extend the magnetomechanical effect

The associate editor coordinating the review of this manuscript and approving it for publication was Jenny Mahoney.

theory are insufficient. Moreover, reports on stress-induced magnetic anisotropy are few and far between [24], [25], and no model was proposed based on experimental data.

This study investigated stress-induced magnetic anisotropy and presented its model under unidirectional stress experiment. First, the theoretical model of the stress-induced magnetic anisotropy was simulated with the J-A model. Second, experiments were conducted, and data were collected and analyzed. Finally, new model was developed by comparing the experimental data with the theoretical model.

## II. THEORETICAL FRAMEWORK

The J-A model was established by Jiles and Atherton based on micro magnetism and Weiss's molecular field theory [1]. According to this model, the effect of stress $\sigma$ on magnetization is equal to the effective magnetic field of $H_\sigma$. The total magnetic field $H_{total}$ is given by

$$H_{total} = H + \alpha M + H_\sigma, \tag{1}$$

$$H_\sigma = \frac{3}{2}\frac{\sigma}{\mu_0}\frac{d\lambda}{dM}, \tag{2}$$

where $H$ is the external magnetic field, $\alpha$ is the coefficient of the magnetic domain coupling, $M$ is the magnetization, $\sigma$ is stress, $\lambda$ is the magnetostriction, and $\mu_0$ is the air permeability.

Given that $\lambda$ is symmetric in $M$, the relationship between magnetostriction $\lambda$ and magnetization $M$ at low magnetization range is given by [26].

$$\lambda = bM^2. \tag{3}$$

This leads to the derivative

$$\frac{d\lambda}{dM} = 2bM, \tag{4}$$

where $b$ is a coefficient that can be determined by using experimental data. Therefore, the effective magnetic field $H_\sigma$ is calculated as follows:

$$H_\sigma = \frac{3\sigma bM}{\mu_0}. \tag{5}$$

When the direction of the principal stress $\sigma_0$ is non-coaxial with the direction of $M$, the stress $\sigma$ in (5) for isotropic materials can be calculated as

$$\sigma = \sigma_0\left(\cos^2\theta - \upsilon\sin^2\theta\right), \tag{6}$$

where $\theta$ is the angle between the principal stress $\sigma_0$ and the magnetic field $H$, and $\upsilon$ is the Poisson's ratio. The equation for the stress-induced magnetic anisotropy model is

$$H_\sigma = \frac{3}{2}\frac{\sigma}{\mu_0}\left(\frac{d\lambda}{dM}\right)_\sigma = \frac{3\sigma_0 bM}{\mu_0}\left(\cos^2\theta - \upsilon\sin^2\theta\right). \tag{7}$$

For simplicity, under a state of unidirectional stress, (6) equals

$$\sigma = \sigma_0\cos^2\theta. \tag{8}$$

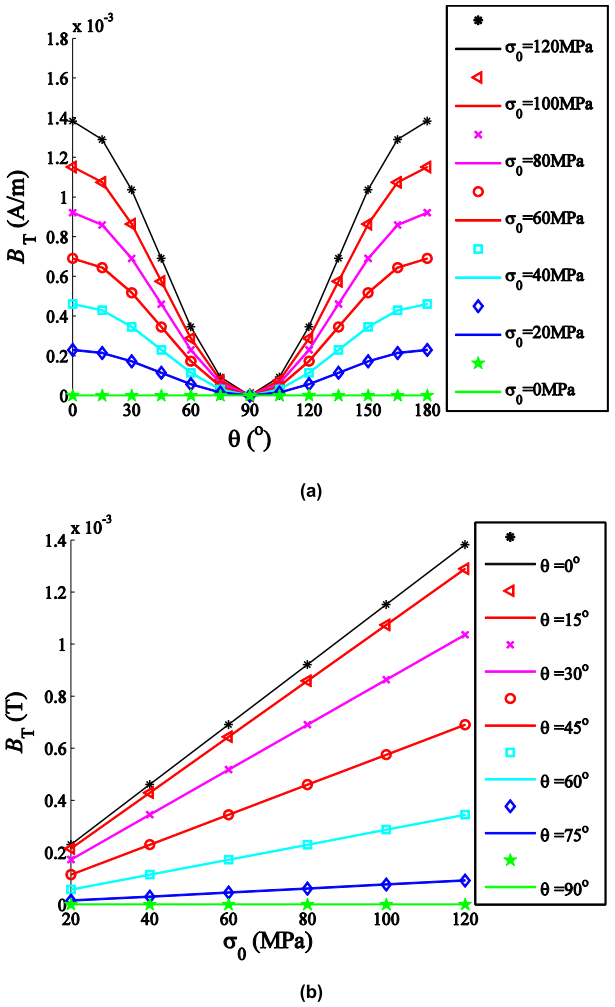


**FIGURE 1.** (a) Relationships between $B_T$ and $\theta$ under different $\sigma_0$ values, where $\sigma_0$ = [0, 20, 40, 60, 80, 100, 120] MPa. (b) Relationships between $B_T$ and $\sigma_0$ under different $\theta$ values, where $\theta$ = [0°, 15°, 30°, 45°, 60°, 75°, 90°], $M = 1.6 \times 10^6$A/m, and $b = 2.4 \times 10^{-18}$(A/m)$^{-2}$.

Therefore, the effective magnetic field $H_\sigma$ under unidirectional stress equals

$$H_\sigma = \frac{3}{2}\frac{\sigma}{\mu_0}\left(\frac{d\lambda}{dM}\right)_\sigma = \frac{3\sigma_0 bM}{\mu_0}\cos^2\theta. \tag{9}$$

The theoretical magnetic field induced by $H_\sigma$, $B_{\mathrm{T}}(\sigma_{0,\theta})$ is

$$B_{\mathrm{T}(\sigma_0,\theta)} = \mu_0 H_\sigma = \frac{3}{2}\sigma\left(\frac{d\lambda}{dM}\right)_\sigma = 3bM\sigma_0\cos^2\theta. \tag{10}$$

According to (10), $B_{\mathrm{T}(\sigma 0,\theta)}$ values for a series of stresses $\sigma_0$ and angles $\theta$ are calculated and shown in Fig. 1, where $B_{T(\sigma 0,\theta)}$ is represented by $B_{\mathrm{T}}$. Fig. 1(a) shows the relationships between $B_{\mathrm{T}}$ and $\theta$ under different $\sigma_0$ values, where $\sigma_0$ = (0,20, 40, 60, 80, 100, 120) MPa. Fig. 1(b) shows the relationships between $B_{\mathrm{T}}$ and $\sigma_0$ under different $\theta$ values, where $\theta$ = (0°, 15°, 30°, 45°, 60°, 75°, 90°). $M$ and $b$ are given values of simulation as $1.6 \times 10^6$A/m and $2.4 \times 10^{-18}$(A/m)$^{-2}$, respectively.

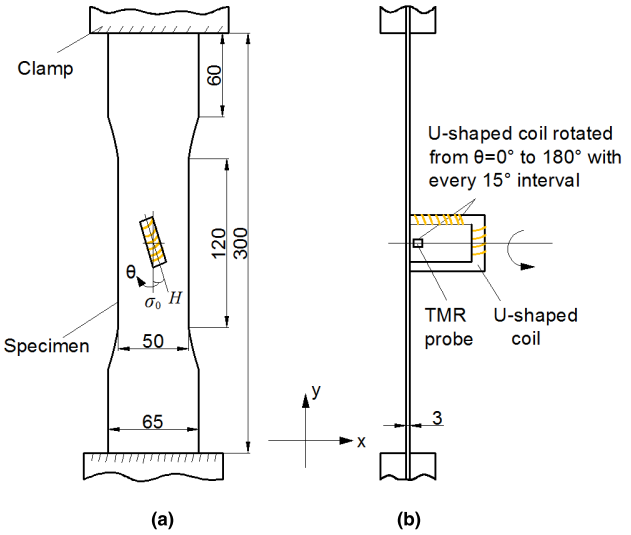


**FIGURE 2.** Shape and size (mm) of the specimen and experiment system (a) Front view, (b) Left view.

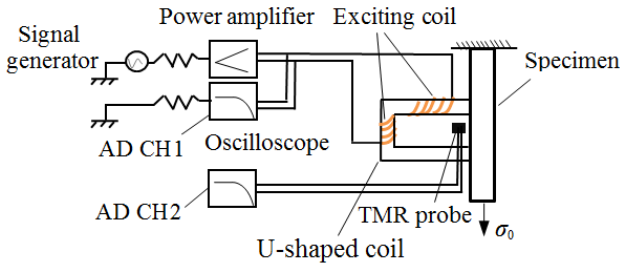


**FIGURE 3.** Magnetic field measurement system.

## III. EXPERIMENTS

The stress-induced magnetic anisotropy model under unidirectional tensile stress was experimentally verified, as shown in Fig. 2. Two specimens fabricated with Q195 ferromagnetic steel and silicon steel were tested. The yield strengths of Q195 and the silicon steel were 195 and 216 MPa, respectively. Fig. 2 shows the shapes and sizes (in mm) of the specimen, TMR probe, and U-shaped coil, where Fig. 2 (a) is the Front view of them, Fig. 2 (b) is the Left view. A series of elastic tensile stress from 0 MPa to 120 MPa, with interval of 20 MPa, was imported into the specimens along the length direction of the specimens with a CMT5305 tensile machine. The principal stress $\sigma_0$ was directed along the length of the specimen. $\theta$ is the angle between the principal stress $\sigma_0$ and magnetic field $H$. At each state of stress, magnetic field $H$ was applied to the specimens in different directions by rotating the U-shaped coil from 0° to 180° with interval of 15°.

Fig. 3 shows the principle diagram of the magnetic field measurement system. A sinusoidal excitation of 300 Hz provided by a signal generator of Puyuan DG4102 and amplified by a power amplifier of NF HSA4014 was imported into a U-shaped coil with 1200 turns coils, which excited a magnetic field and imported it into the specimen. The exciting magnetic field $H$ and the induced magnetic field $B$ sensed by a tunneling magnetoresistance probe were collected by the AD CH1 and AD CH2 channels of a Puyuan DS4014 oscilloscope, respectively.

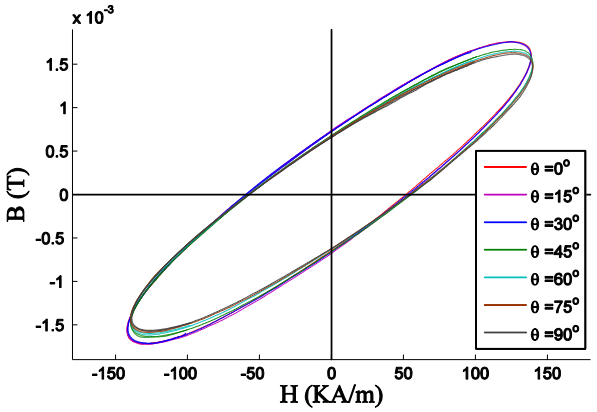


**FIGURE 4.** Magnetic hysteresis loops (*B-H* curves) of Q195 specimen with angles $\theta$ from 0° to 90° under a stress of 60 MPa.

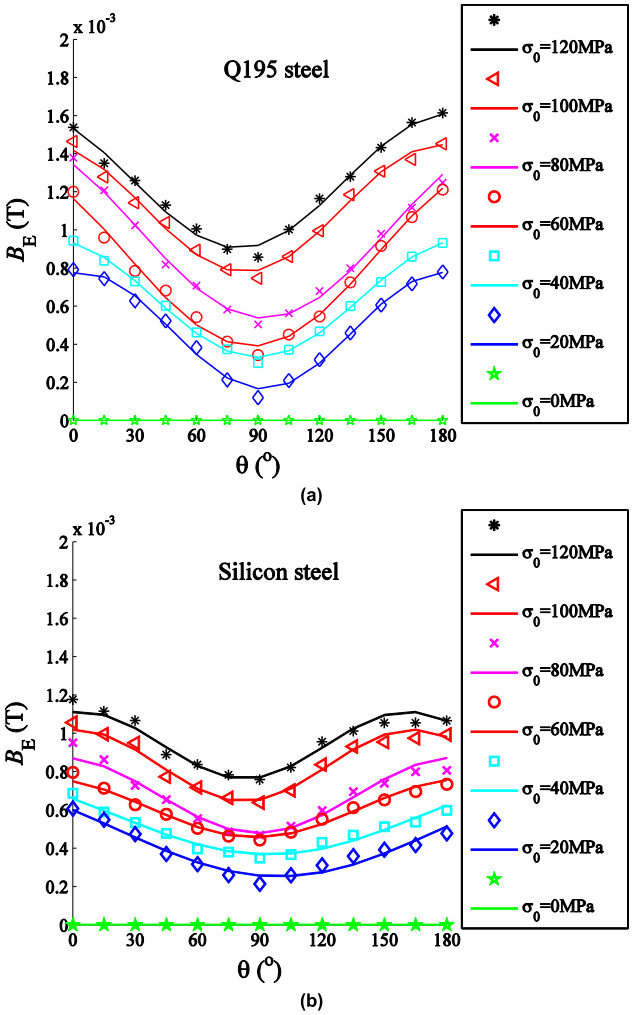


**FIGURE 5.** Relationships between $B_E$ and $\theta$ with different $\sigma_0$ values of (a) Q195 steel and (b) silicon steel, where $\sigma_0$ = (0, 20, 40, 60, 80, 100, 120) MPa, (*,◁,×,○,□,◇) = experimental data, solid lines = fitting lines.

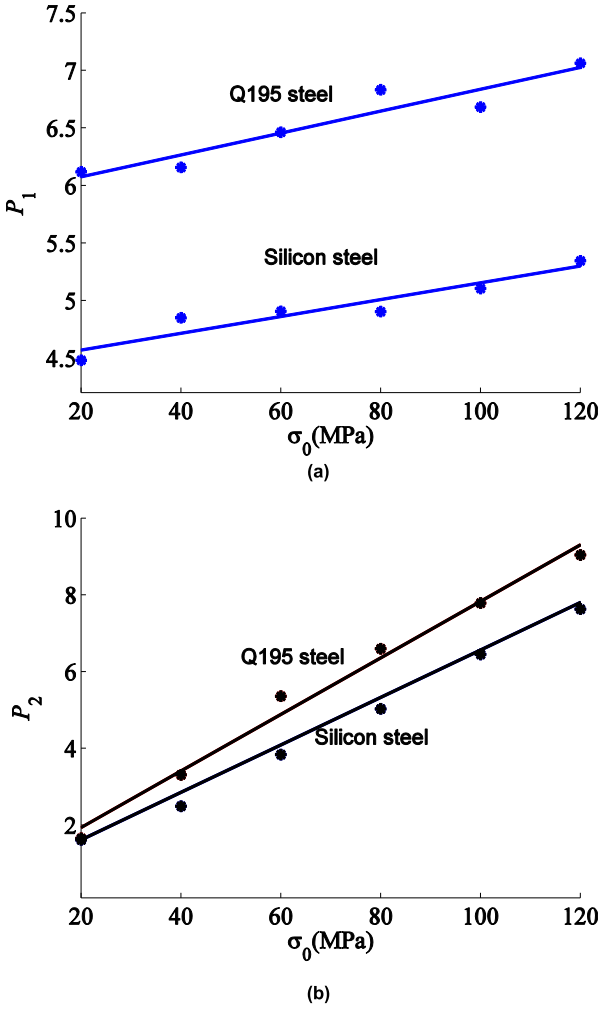


**FIGURE 6.** Relationships between parameters of (a) $P_1$, (b) $P_2$, and stress $\sigma_0$, where [*] = experimental data, solid lines = fitting lines.

A series of $B$-$H$ curves in 0°–180° angles under stresses of 0–120 MPa of the two specimens was collected. Fig. 4 shows the $B$-$H$ curves of the Q195 specimen with angle $\theta$ from 0° to 90° under stress of 60 MPa.

## IV. ANALYSIS AND DISCUSSION

Fig. 4 shows the $B$-$H$ curves change with the angles of $\theta$. The experimental values of $B$ under the action of the maximum $H$ ($H_{max}$) of all $B$-$H$ curves were extracted for the comparison of the variations of $B$ in different angles and stresses and summarization of the change law of $B$ with angle $\theta$ and stress $\sigma_0$. All extracted $B$ values subtracted the extracted $B$ values of 0 MPa, and the experimental $B_E$ under $H_{max}$ induced by stress was obtained.

The susceptibility $\chi$ value changes with the intensity of the exciting magnetic field $H$ in ferromagnetic materials, such as Q195 steel and silicon steel, but the susceptibility $\chi$ values under $H_{max}$ are the same in theory because the $H_{max}$ values for all $B$-$H$ curves are constant. In the magnetization $M = \chi H$, the $M$ values excited by the $H_{max}$ for all $B$-$H$ curves are the same. According to (10), the experimental $B_E$ induced by

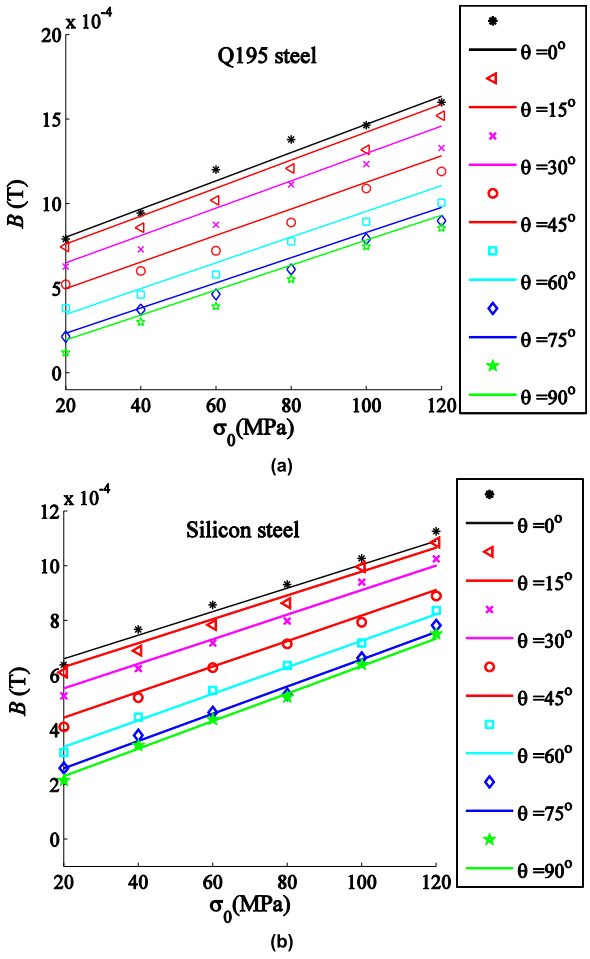


**FIGURE 7.** Relationship between $B$ and stress $\sigma_0$ under different angles $\theta$ of (a) Q195 steel, (b)Silicon steel, where [*,◁,×,○,□,◇] = experimental data, solid lines = calculated results by developed model.

stress mainly changes with stress $\sigma_0$ and angle $\theta$. Fig. 5 shows the relationships between $B_E$ and $\theta$ under the different $\sigma_0$ values of the two specimens, where $\sigma_0$ = (0, 20, 40, 60, 80, 100, 120) MPa.

The experimental data in Fig. 5 are shown in a cosine form, so the experimental data $B_E$ induced by stress can be described as

$$B_E = P_1 \cos^2 \theta + P_2, \tag{11}$$

where $P_1$ and $P_2$ are the fitting parameters. The relationship between parameters $P_1$, $P_2$, and stress $\sigma_0$ is shown in Fig. 6 for the exploration of $P_1$ and $P_2$ correlations with stress $\sigma_0$.

Fig. 6 shows parameters $P_1$ and $P_2$ have good linear relation with stress $\sigma_0$. Therefore, parameters $P_1$ and $P_2$ can be formulated with stress $\sigma_0$ as

$$P_1 = a_1\sigma_0 + b_1, \tag{12}$$

$$P_2 = a_2\sigma_0 + b_2, \tag{13}$$

where $a_1$, $b_1$, $a_2$, and $b_2$ are fitting parameters. In Q195, $a_1 = 0.0095$, $b_1 = 5.8865$, $a_2 = 0.0737$, and $b_2 = 0.4640$. In silicon steel, $a_1 = 0.0073$, $b_1 = 4.4244$, $a_2 = 0.0619$, and $b_2 = 0.3791$.

Substituting (12) and (13) into (11), the following equation can be obtained:

$$B_{\mathrm{E}(\sigma_0,\theta)} = a_1\sigma_0\cos^2\theta + a_2\sigma_0 + b_1\cos^2\theta + b_2. \quad (14)$$

Recombining (14) in the form of (10), the following equation can be obtained:

$$B_{(\sigma_0,\theta)} = 3bM\sigma_0\left(\cos^2\theta + C\right) + b_1\cos^2\theta + b_2, \quad (15)$$

where $M$ can be calculated by $B_E$ and $H_{\max}$, $M = B_E/\mu_0$-$H_{max}$, $M = 9.18 \times 10^8$A/m for Q195 steel, and $M = 1.2 \times 10^9$A/m for silicon steel. $b$ can be calculated by $b = a_1/3M$, $b = 3.4 \times 10^{-12}(\mathrm{A/m})^{-2}$ for Q195 steel and $b = 2.0 \times 10^{-12}(\mathrm{A/m})^{-2}$ for silicon steel. $C = a_2/3\ bM$, $C = 7.7579$ for Q195 steel, and $C = 8.4795$ for silicon steel.

According to the comparison between (15) and (10), the experimental model (15) involves two terms, 3 $bM(\cos{}^2\theta + C)\sigma_0$ and $b_1\cos{}^2\theta + b_2$, which describe the stress-induced magnetic anisotropy of ferromagnetic materials. The stress-induced magnetic field $B$ excited by $H_{max}$ was calculated by using the developed model in (15). Fig. 7 shows the relationship between $B$ and stress $\sigma_0$, and $B$ increased almost linearly with increasing the stress. Thus, we can quantitatively evaluate the stress by $B$. Fig. 7 also indicates that the calculated results used in (15) are consistent with the experimental results. This finding verifies the correctness of the developed model of stress-induced magnetic anisotropy under unidirectional tension.

## V. CONCLUSIONS

A stress-induced magnetic anisotropy model under unidirectional tensile stress was developed by connecting experimental data with the theoretical model. The fact that the experimental results match very well with the results obtained from the model implies the validity of the stress-induced magnetic anisotropy model reported in this paper. These results also lay a foundation for the quantitative testing and evaluation of stress of ferromagnetic materials through the magnetic method.

## REFERENCES


[1] D. C. Jiles, "Theory of the magnetomechanical effect," *J. Phys. D, Appl. Phys.*, vol. 28, no. 8, pp. 1537–1546, Aug. 1995.

[2] A. A. Dubov, "A study of metal properties using the method of magnetic memory," *Metal Sci. Heat Treat.*, vol. 39, no. 9, pp. 401–405, Sep. 1997.

[3] D. C. Jiles, "Review of magnetic methods for nondestructive evaluation," *NDT Int.*, vol. 21, no. 5, pp. 311–319, 1988.

[4] M. Rebican, Z. Chen, N. Yusa, L. Janousek, and K. Miya, "Shape reconstruction of multiple cracks from ECT signals by means of a stochastic method," *IEEE Trans. Magn.*, vol. 42, no. 4, pp. 1079–1082, Apr. 2006.

[5] Z. Chen, M. Rebican, N. Yusa, and K. Miya, "Fast simulation of ECT signal due to a conductive crack of arbitrary width," *IEEE Trans. Magn.*, vol. 42, no. 4, pp. 683–686, Apr. 2006.

[6] D. C. Jiles and D. L. Atherton, "Theory of the magnetisation process in ferromagnets and its application to the magnetomechanical effect," *J. Phys. D, Appl. Phys.*, vol. 17, no. 12, pp. 1265–1281, Dec. 1984.

[7] S. Ren and X. Ren, "Studies on laws of stress-magnetization based on magnetic memory testing technique," *J. Magn. Magn. Mater.*, vol. 449, pp. 165–171, Mar. 2018.

[8] S. Ren, X. Ren, Z. Duan, and Y. Fu, "Studies on influences of initial magnetization state on metal magnetic memory signal," *NDT E Int.*, vol. 103, pp. 77–83, Apr. 2019.

[9] H. Huang, S. Jiang, C. Yang, and Z. Liu, "Stress concentration impact on the magnetic memory signal of ferromagnetic structural steel," *NDT E Int.*, vol. 29, no. 4, pp. 377–390, Oct. 2014.

[10] S. G. H. Staples, C. Vo, D. M. J. Cowell, S. Freear, C. Ives, and B. T. H. Varcoe, "Solving the inverse problem of magnetisation–stress resolution," *J. Appl. Phys.*, vol. 113, no. 13, Apr. 2013, Art. no. 133905.

[11] L. Zhong, L. Li, and X. Chen, "Simulation of magnetic field abnormalities caused by stress concentrations," *IEEE Trans. Magn.*, vol. 49, no. 3, pp. 1128–1134, Mar. 2013.

[12] J. Li and M. Xu, "Modified Jiles-Atherton-Sablik model for asymmetry in magnetomechanical effect under tensile and compressive stress," *J. Appl. Phys.*, vol. 110, no. 6, Sep. 2011, Art. no. 063918.

[13] M. X. Xu, M. Q. Xu, J. W. Li, and H. Y. Xing, "Using modified J–A model in MMM detection at elastic stress stage," *NDT E Int.*, vol. 27, no. 2, pp. 121–138, 2012.

[14] J. Li, M. Xu, J. Leng, M. Xu, and S. Zhao, "Metal magnetic memory effect caused by circle tensile-compressive stress," *Insight Non-Destructive Test. Condition Monit.*, vol. 53, no. 3, pp. 142–145, Mar. 2011.

[15] P. Shi, K. Jin, P. Zhang, S. Xie, Z. Chen, and X. Zheng, "Quantitative inversion of stress and crack in ferromagnetic materials based on metal magnetic memory method," *IEEE Trans. Magn.*, vol. 54, no. 10, pp. 1–11, Oct. 2018.

[16] P. Shi, P. Zhang, K. Jin, Z. Chen, and X. Zheng, "Thermo-magneto-elastoplastic coupling model of metal magnetic memory testing method for ferromagnetic materials," *J. Appl. Phys.*, vol. 123, no. 14, Apr. 2018, Art. no. 145102.

[17] K. Wang, S. Xie, S. Li, P. Shi, S. Tian, and Z. Chen, "Evaluation of electromagnetic force in tokamak first wall based on magnetic field measurement and inverse analysis," *Int. J. Appl. Electromagn. Mech.*, vol. 59, no. 2, pp. 427–437, Mar. 2019.

[18] B. D. Cullity and C. D. Graham, *Introduction to Magnetic Materials*. Reading, MA, USA: Addison-Wesley, 1972.

[19] B. Yang, H. Li, and A. Zhang, "Influences of non-coaxial magnetic field on magneto-mechanical effect of ferromagnetic steel," *Int. J. Appl. Electromagn.*, vol. 59, no. 1, pp. 247–254, Mar. 2019.

[20] H. Li and Z. Chen, "Quantitative analysis of the relationship between non-uniform stresses and residual magnetizations under geomagnetic fields," *AIP Adv.*, vol. 6, no. 7, Jul. 2016, Art. no. 075309.

[21] H. Li, Z. Chen, D. Zhang, and H. Sun, "Reconstruction of magnetic charge on breaking flaw based on two-layers algorithm," *Int. J. Appl. Electromagn.*, vol. 52, nos. 3–4, pp. 1133–1139, Dec. 2016.

[22] H. Li, L. Wang, Y. Li, D. Zhang, and Z. Chen, "Reconstruction of damage-induced magnetization with leakage magnetic field signals," *Int. J. Appl. Electromagn.*, vol. 39, nos. 1–4, pp. 221–227, Sep. 2012.

[23] L. Sun, X. Liu, D. Jia, and H. Niu, "Three-dimensional stress-induced magnetic anisotropic constitutive model for ferromagnetic material in low intensity magnetic field," *AIP Adv.*, vol. 6, no. 9, Sep. 2016, Art. no. 095226.

[24] C. Rizal, P. Gyawali, I. Kshattry, and R. K. Pokharel, "Strain-induced magnetoresistance and magnetic anisotropy properties of Co/Cu multilayers," *J. Appl. Phys.*, vol. 111, no. 7, Apr. 2012, Art. no. 07C107.

[25] S. Florez and R. Gomez, "Strain-induced resistance changes in CoFe/CuGMR multilayers," *IEEE Trans. Magn.*, vol. 39, no. 5, pp. 3411–3413, Sep. 2003.

[26] P. Garikepati, T. T. Chang, and D. C. Jiles, "Theory of ferromagnetic hysteresis: Evaluation of stress from hysteresis curves," *IEEE Trans. Magn.*, vol. MAG-24, no. 6, pp. 2922–2924, Nov. 1988.


**FUCHEN ZHANG** received the B.S. and M.S. degrees in applied physics and mechanical—electronic engineering from Northeast Petroleum University, Daqing, China, in 2008 and 2011, respectively. He is currently pursuing the Ph.D. degree with the School of Mechanical Electronic and Information Engineering, China University of Mining and Technology, Beijing. His research interests are stress-induced magnetic anisotropy, electromagnetic nondestructive testing, and magnetically measured stress and their industrial applications.

**HONGMEI LI** received the B.S. degree in mechanical engineering from Jilin University, Changchun, China, in 1997, and the M.S. and Ph.D. degrees in mechanical engineering and engineering mechanics from Xi'an Jiaotong University, Xi'an, China, in 2006 and 2012, respectively.

She is currently a Professor, a Ph.D. Supervisor, and the Vice Dean with the School of Mechanical Engineering, North Minzu University, Yinchuan. Her current research interests include magneto-mechanical effect, electromagnetic non-destructive testing, electromagnetic inverse problem, and their industrial applications. She was a recipient of the Young Excellent Talents in the State Ethnic Affair Commission of China.

**CHENGXIANG SHI** received the B.S. degree in electronic and information engineering from Lvliang University, lvliang, China, in 2018. He is currently pursuing the master's degree in circuits and systems with North Minzu University, Yinchuan, China. His research interests are stress-induced magnetic anisotropy and electromagnetic nondestructive testing.

**RUIQING JIA** received the M.S. and Ph.D. degrees from the China University of Mining and Technology, Beijing, China, in 1989 and 1992, respectively.

He is currently a Professor and a Ph.D. Supervisor with the School of Mechanical Electronic and Information Engineering, China University of Mining and Technology, Beijing. His current research interests include intelligent manufacturing systems and MEMS.